Stochastic cyclotron resonance in semiconductors with nonparabolic bands

K. A. Piragas

Institute of Semiconductor Physics, Lithuanian Academy of Sciences
(Submitted 30 November 1984)
Zh. Eksp. Teor. Fiz. **88**, 2258–2263 (June 1985)

Cyclotron resonance in semiconductors with nonparabolic dispersion law is investigated in the balance-equation approximation. It is shown that at sufficiently large amplitudes of the external high-frequency field the system has stochastic behavior. This behavior leads to a dip of the frequency characteristic of the absorption coefficient (to clearing of the sample), and the high-frequency field radiated by the sample is an aperiodic noiselike signal with a continuous spectrum.

1. INTRODUCTION

Levinson and Shvarts[1] investigated in the balance-equation approximation cyclotron resonance in nonparabolic-band semiconductors and have demonstrated the possible existence of hysteresis in the frequency dependence of the absorption coefficient. This effect is connected with the dependence of the cyclotron frequency on the electron-orbit radius in momentum space. Since the initial equations of the model correspond to the motion of an anharmonic oscillator perturbed by a periodic external field, the effect indicated constitutes in essence the well known property of nonlinear resonance. The solution obtained in Ref. 1 is exact only for a circularly polarized electromagnetic wave. In the case of low amplitudes of the external field (weak nonlinearity) this solution naturally remains valid also for arbitrary polarization.

The present paper deals with absorption and emission of electromagnetic waves by a semiconductor with nonparabolic dispersion law for high amplitudes of the external field (strong nonlinearity). In contrast to Ref. 1, linear polarization is dealt with here. In this formulation, the problem is of interest from the viewpoint of the stochastic behavior recently observed in a number of systems that constitute nonlinear oscillators perturbed by a periodic external force.[2–5] The purpose of the present paper is to shed light on the possible existence of such a regime in cyclotron resonance, and to investigate its manifestations in various physical characteristics.

2. BALANCE EQUATIONS AND THEIR ANALYTIC INVESTIGATION

The balance equation for the momentum components p_x and p_y transverse to the magnetic field are[1]

$$dp_x/dt=-p_y\Omega(p)-p_x/\tau, \quad dp_y/dt=p_x\Omega(p)-p_y/\tau-eE\sin\omega t, \tag{1}$$

where τ is the momentum relaxation time, Ω is the cyclotron frequency, e is the electron charge, and E and ω are the amplitude and frequency of an external high-frequency electric field. In the case of a nonparabolic but isotropic dispersion law, Ω depends only on the modulus of the momentum:

$$\Omega=\frac{eB}{p}\frac{d\varepsilon}{dp}, \quad p=(p_x^2+p_y^2)^{1/2}. \tag{2}$$

The constant magnetic field B is assumed here directed along the z axis, and the high-frequency electric field is polarized along the y axis. The criteria for the applicability of these equations are given in Ref. 1.

Assuming that the dispersion law is that given by Kane,[6] we obtain for the square of the cyclotron frequency the Lorentz relation $\Omega^2(p)=\Omega_0^2/(1+p^2/p_0^2)$, where $\Omega_0=eB/m$ is the cyclotron frequency on the bottom of the band, m is the effective mass on the bottom of the band $p_0=(m\varepsilon_g/2)^{1/2}$ is the momentum that characterizes the nonparabolicity, and ε_g is the band gap. To simplify the analysis that follows, we replace the Lorentz function by the Heaviside step function:

$$\Omega(p)=\Omega_0\theta(p_0-p)\equiv\begin{cases}\Omega_0, & p<p_0\\ 0, & p>p_0\end{cases}. \tag{3}$$

Changing next to dimensionless variables

$$p_x\Omega_0/eE\to p_x, \quad p_y\Omega_0/eE\to p_y, \quad p\Omega_0/eE\to p=(p_x^2+p_y^2)^{1/2},$$
$$p_0\Omega_0/eE\to p_0\equiv B(\varepsilon_g/2m)^{1/2}/E, \quad \omega/\Omega_0\to\omega, \quad \tau\Omega_0\to\tau, \quad t\Omega_0\to t, \tag{4}$$

we obtain the following system of piecewise-linear equations:

$$dp_x/dt=-p_y\theta(p_0-p)-p_x/\tau,$$
$$dp_y/dt=p_x\theta(p_0-p)-p_y/\tau-\sin\omega t. \tag{5}$$

It is convenient to write the solution of these equations in each of the momentum-space regions $p<p_0$ and $p>p_0$ for the complex momentum $q=p_x+ip_y$, $|q|=p$:

$$q=\frac{e^{-i\omega t}}{2\{1/\tau-i(\omega+1)\}}-\frac{e^{i\omega t}}{2\{1/\tau+i(\omega-1)\}}+C_1e^{it-t/\tau}, \quad |q|<p_0; \tag{6}$$

$$q=\frac{e^{-i\omega t}}{2(1/\tau-i\omega)}-\frac{e^{i\omega t}}{2(1/\tau+i\omega)}+C_2e^{-t/\tau}, \quad |q|>p_0, \tag{7}$$

where the constants C_1 and C_2 are determined from the condition that these solutions be matched at the boundary $|q|=p_0$ of the indicated regions. Expressions (6) and (7) constitute a sum of three oscillations: the first two are induced harmonic oscillations in counterphase, having the frequency ω of the external force, and the third is a natural damped oscillation of unity or zero frequency, depending on the value of $|q|$. Whenever the amplitude of the combined oscillation reaches $|q|=p_0$, a jumplike change of the amplitudes of

 0038-5646/85/061335-04$04.00

the component oscillations takes place, and furthermore in such a way that the resultant oscillation proceeds continuously. At certain values of the parameters, the steady-state combined oscillation take place wholly in the region $|q| < p_0$. In this case the solutions of Eqs. (5) can be obtained analytically. In fact, the oscillation that is in the steady state in the region $|q| < p_0$ is described by the first two terms of expression (6), and these terms correspond in the complex q plane to motion of the representative point along an ellipse. The condition for this ellipse to be located in the region $|q| < p_0$, and hence the condition that solution (6) is valid, takes for an arbitrary time the form

$$\{(\omega-1)^2+1/\tau^2\}^{-1/2}+\{(\omega+1)^2+1/\tau^2\}^{-1/2}<2p_0. \quad (8)$$

When this inequality holds it is easy to calculate, using (6), various physical characteristics of the system. Of definite interest for the subsequent investigation are the frequency characteristics of the absorption coefficient $K(\omega) \propto \langle \theta(p_0 - |q|)\mathrm{Im}q \sin\omega t \rangle$ (the angle brackets denote averaging over the time) and of the steady-state stroboscopic (at each period of the external force) value of the amplitude $q_n(\omega)$. If Eq. (8) is satisfied, the expressions for them are:

$$K(\omega)\sim\{(\omega-1)^2+1/\tau^2\}^{-1}+\{(\omega+1)^2+1/\tau^2\}^{-1}, \quad (9)$$

$$q_n(\omega)=i\omega/(\omega^2-1+1/\tau^2-i2/\tau). \quad (10)$$

In the case $1 \ll \tau < 2p_0$ the inequality (8) is satisfied for arbitrary frequencies and expressions (9) and (10) yield the complete frequency characteristics of the investigated quantities. At $\tau > 2p_0$, i.e., at sufficiently large amplitudes of the high-frequency field, the condition (8) is not satisfied in a definite frequency interval. To construct the trajectory of Eqs. (5) it is necessary in this case to match numerically the solutions (6) and (7).

3. RESULTS OF NUMERICAL ANALYSIS

The presence of simple analytic solutions in individual regions of phase space shortens substantially the computer calculations not only of the dynamics of the system, but also of such integral characteristics as the absorption coefficient and the spectral density of the signal, since the corresponding integrals can be evaluated analytically in individual regions and the task of the computer reduces to summing their contributions at the matching points. The calculation results are shown in Figs. 1–3. The order of magnitude of the chosen parameters is the same as in Ref. 1, $p_0 = 3$ and $\tau = 10$. In terms of the initial variables these correspond for n-InSb to the following choice: $m = 0.013m_0$, $\varepsilon_g = 0.23$ eV, $\tau = 10^{-11}$ s, $B = 740$ G, $E = 300$ V/cm, and $\Omega_0 = 10^{12}\mathrm{s}^{-1}$. At these values of the parameters the condition (8) is not satisfied in the next frequency interval: $0.85 < \omega < 1.15$. It turns out that in practically this entire interval the system investigated exhibits a stochastic behavior, as can be seen from Fig. 1, which shows the frequency characteristic of the stroboscopic transformation of the modulus of the momentum $p_n(\omega) = |q_n(\omega)|$. The plot was constructed in the following manner. The fre-

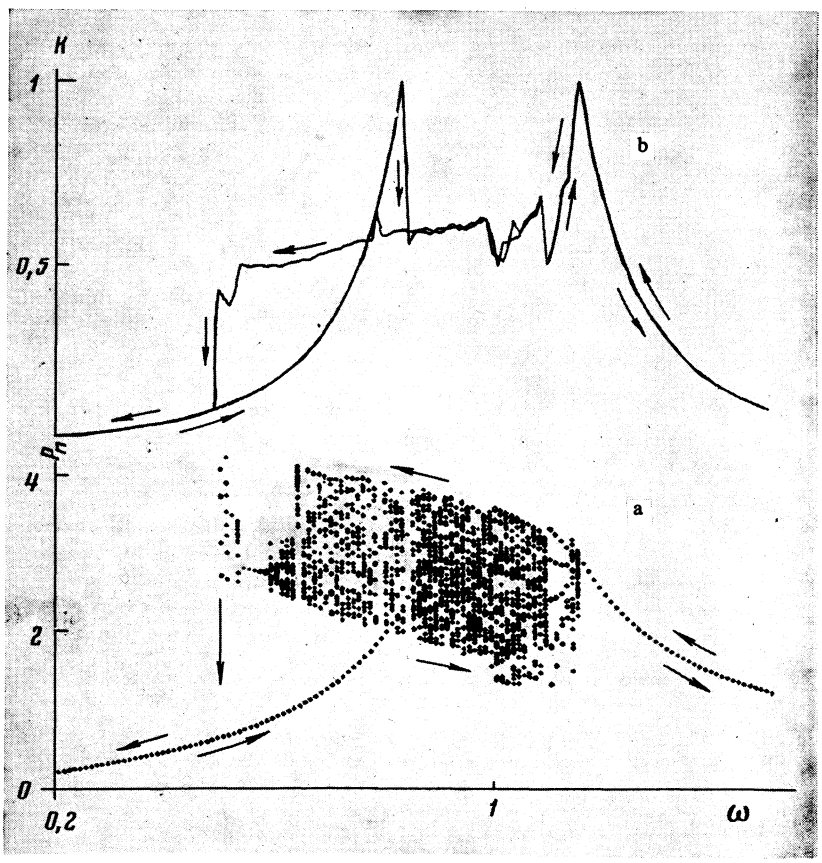

FIG. 1. Frequency characteristics of the stroboscopic transformation of the modulus of the momentum (a) and of the absorption coefficient (b).

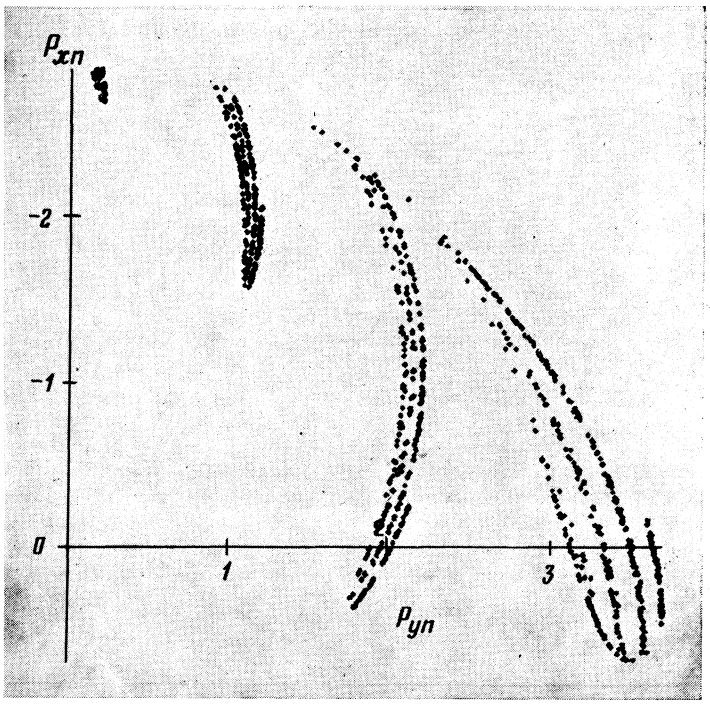

FIG. 2. Stroboscopic portrait of system in the total phase plane at $\omega = 0.9$.

quency was varied from an initial value $\omega = 0.2$ in steps $\Delta\omega = 0.01$ first upward to $\omega = 1.5$ and then downward to the initial value. At each change of frequency, the initial values of $q_n(\omega)$ were taken to be the final values of the preceding transformation $q_n(\omega \mp \Delta\omega)$. This was followed by calculating 200 idle periods and then marking on the diagram 20 stroboscopic $p_n(\omega)$ points. It can be seen from the figure that stochastic dynamics is observed not only in the frequency band $0.85 < \omega < 1.15$ indicated above, when the phase trajectroy must cross the circle $|q| = p_0$, but also in the region $0.5 < \omega < 0.85$, where the solution (10) is valid. Such a second solution is obtained in this region when the frequency is lowered from the region with the stochastic dynamics. We note that in the region with purely stochastic dynamics the solution is not single-valued, since the stroboscopic phase portrait depends on initial conditions that are connected with the direction in which the frequency changes. Besides the stochastic dynamics, the figure shows also the frequency region where multiperiodic cycles are realized. Thus, two three-period cycles with different frequency-change directions are present in the region $1.09 < \omega < 1.12$. All in all, diagram 1a recalls the stochastically smeared amplitude-frequency characteristic of a weakly linear oscillator.

The bifurcation observed in the system dynamics when the frequency is measured is carried over also to the absorption, and leads to a nonmonotonic (at times with fine structure) dependence of the absorption coefficient (Fig. 1b). In the calculation of $K(\omega)$, the power absorbed by the sample was averaged over 200 periods of the external field. Further increase of the averaging interval did not affect the calculation result. An important factor in the frequency characteristic of the absorption coefficient is the dip in the frequency region close to resonance, where a linear or weakly linear oscillator has maximum absorption. The considerable decrease of the absorption of a strong high-frequency field (clearing of the sample) is due here to the stochastic character of the current in the sample. This effect is probably a universal property of strongly nonlinear non-autonomous oscillators in their stochastic regime and can serve as a good indicator of such a regime.

For a more detailed illustration of the stochastic regime in the investigated system, Figs. 2 and 3 show, for the particular frequency $\omega = 0.9$, the stroboscopic phase protrait of

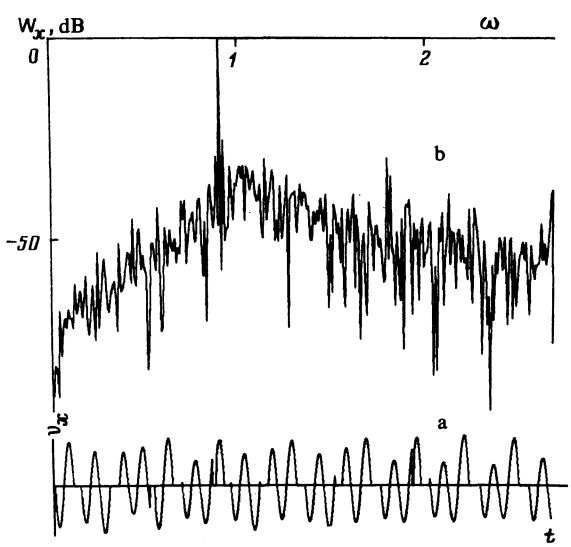

FIG. 3. Temporal realization of the velocity x-component v_x (a) and spectral density of radiation power in a polarization vertical to the external field (b): $\omega = 0.9$.

q_n in the total p_x, p_y phase plane, as well as the temporal realization of the velocity $v_x \sim p_x \theta(p_0 - p)$ and the spectrum of its derivative. The phase portrait in Fig. 2 is made up of 100 stroboscopic points, which outline the contours of the strange attractor that is realized here. The best way to observe directly the stochastic dynamics is by the sample radiation in a polarization vertical to the external field. The measured quantity in this case can be the spectral density of the radiation power $W_x(\omega)$, which is proportional to the spectral density of the derivative of the $v_x(t)$ signal. The spectrum shown in Fig. 3b was obtained by expanding the derivative of the $v_x(t)$ signal in a Fourier series over an interval equal to 200 periods of the external field. It can be seen from the figure that besides the sharp peak at the external-field frequency $\omega = 0.9$ the sample radiates in a wide frequency range a practically continuous spectrum. Approximately 10% of the signal energy goes into the continuum, i.e., the energy of the harmonic high-frequency field is converted quite effectively into noise energy.

The author is grateful to V. L. Bonch-Bruevich, I. B. Levinson, and A. Yu. Matulis for a discussion of the results.

[1]I. B. Levinson and M. L. Shvarts, Pis'ma Zh. Eksp. Teor. Fiz. **6**, 981 (1967) [JETP Lett. **6**, 393 (1967)].
[2]K. Tomita and T. Kai, Progr. Theor. Phys. Suppl. **64**, 280 (1978).
[3]T. Tomita, Phys. Reports **86**, 113 (1982).
[4]B. A. Huberman and J. P. Crutchfield, Phys. Rev. Lett. **43**, 1742 (1979).
[5]R. W. Leven and B. P. Koch, Phys. Lett. **86A**, 71 (1981).
[6]E. O. Kane, J. Phys. Chem. Sol. **1**, 249 (1957).

Translated by J. G. Adashko